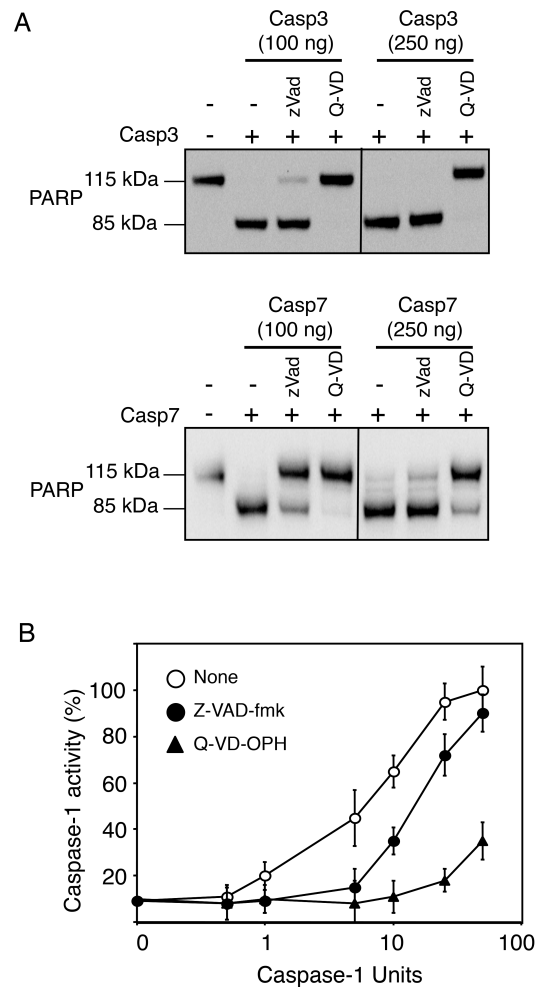
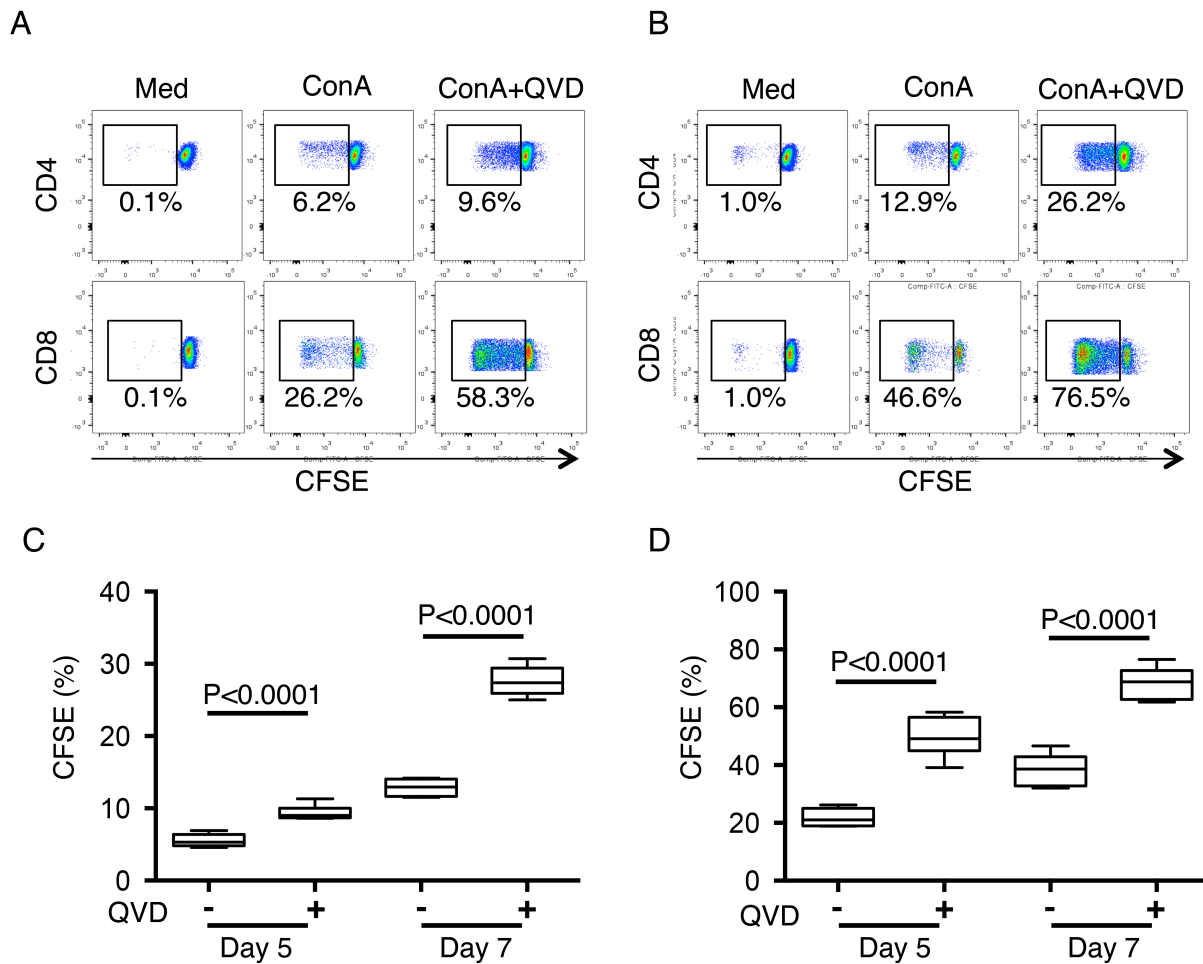


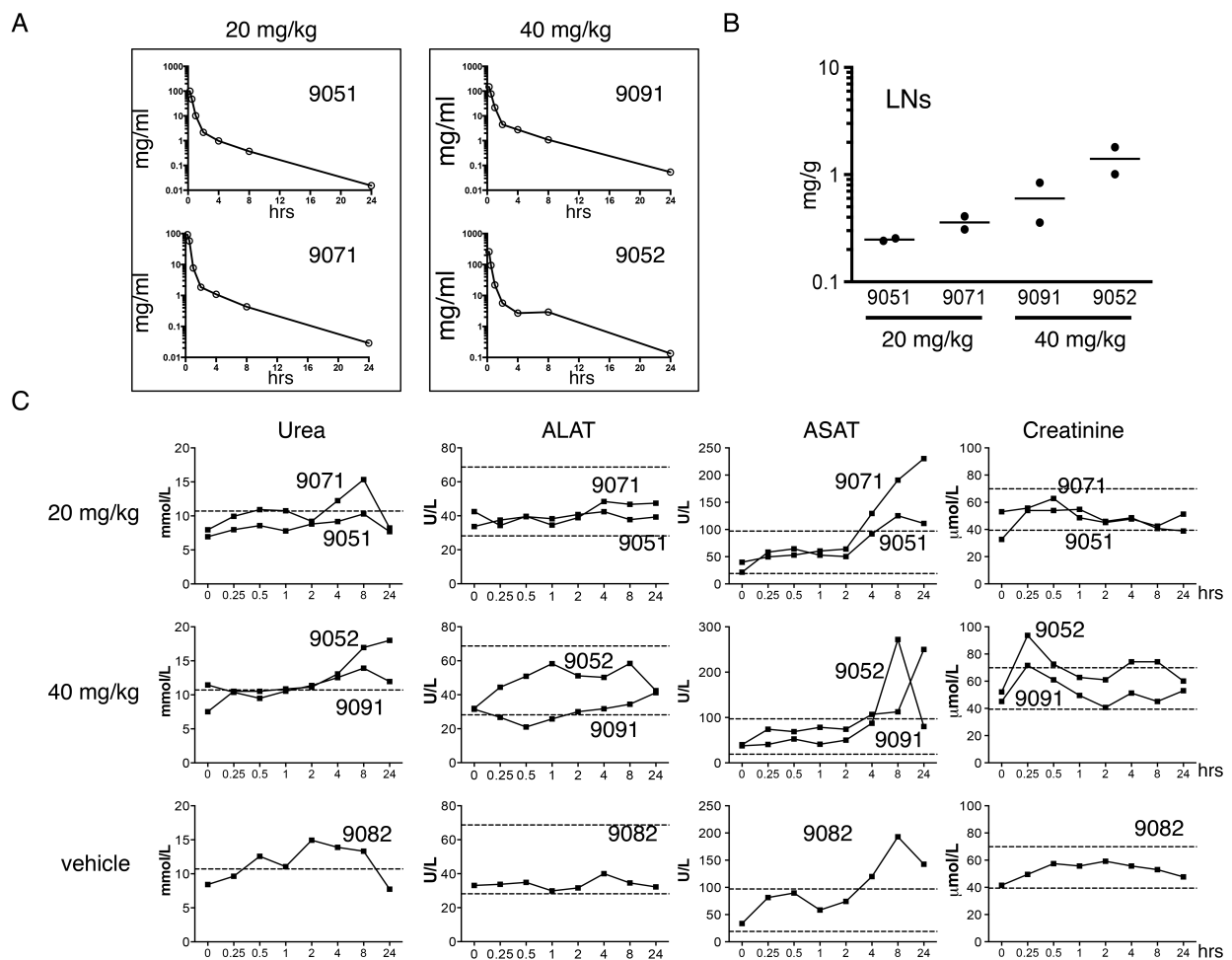
Supplemental Figure 1: Q-VD-OPH inhibits caspase activity. (A) Q-VD blocks caspase-3 and caspase-7 activities in a cell-free system. Recombinant Caspase-3 (casp3), caspase-7 (casp7), and PARP were purchased from R&D System (Mineapolis, MN, USA). Caspases, at the doses of 100 ng/ml and 250 ng/ml, were incubated with PARP, in the absence or presence of either zVAD-fmk (25 μ M) or Q-VD-OPH (25 μ M). After 45 minutes, proteins were loaded on acrylamid gel. Western blots were then visualized using a mouse monoclonal anti-PARP (C2-10; Pharmingen), and horseradish peroxidase-conjugated secondary antibodies (Amersham Biosciences, Inc.). Western blots were visualized by enhanced chemiluminescence method (ECL⁺ from GE Healthcare), and a CCD camera (GBOX, SYNGENE). The cleaved form of PARP has a 85 kDa molecular weight. Q-VD-OPH is more potent to block caspase-3 and caspase-7 than zVAD-fmk. The lanes were run on the same gel but were noncontiguous (B) Caspase-1 (ICE) Assay (Enzo Life Sciences). Recombinant caspase-1 is incubated with Ac-YVAD-pNA colorimetric substrate (200 μ M). Absorbance was measured at A405 nm. The reaction was performed in the absence (None) or presence of either zVAD-fmk (10 μ M) or Q-VD-OPH (10 μ M).



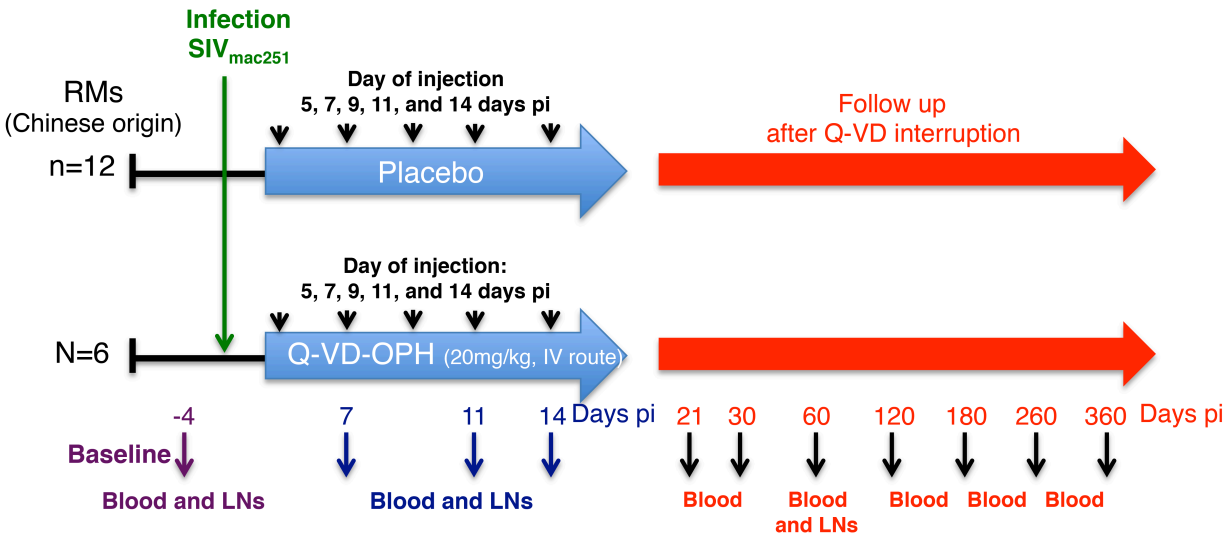
Supplemental Figure 2: Q-VD-OPH enhances T cell proliferation. To monitor cell division and proliferation, cells were labeled with CFSE (1 μ M/ml, Invitrogen). Cells were incubated for 10 minutes at room temperature in the dark. Labeling was stopped by adding 4-5 volumes of cold complete media and incubated on ice for 5 minutes. Representative flow cytometric analysis of the proliferative capacity of CFSE-labelled CD4⁺ and CD8⁺ T cells of a SIV-infected RM. (A, B) Cells were cultured in the absence (Med) or presence of ConA (5 μ g/ml) in the absence or presence of Q-VD-OPH. ConA is a well-known activator for T cells in non-human primates, and early described (1). The ddl was added in the culture to inhibit viral replication. Indeed, in its absence, T cell stimulation may lead to viral production, which in turn may affect cell survival. Therefore, this experimental step is essential to assess T cell proliferation during *in vitro* culture of T cells derived from SIV-infected monkeys (2). CFSE staining was assessed in CD4 and CD8 T cells by flow cytometry at days 5 (B) and 7 (C). Statistical significance was assessed using paired Student's *t*-test.



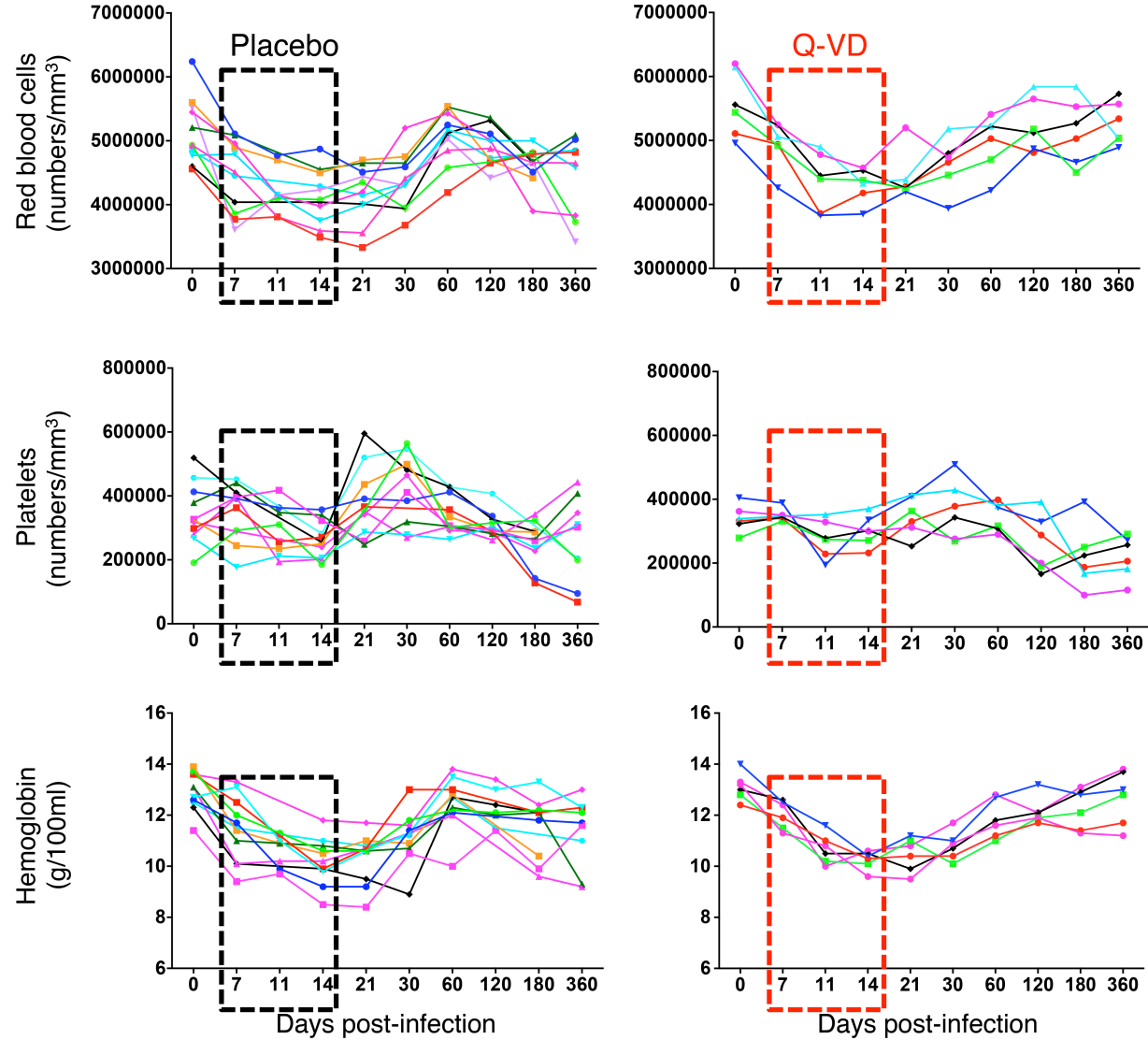
Supplemental Figure 3: Q-VD pharmacokinetic profile in RMs: (A) Q-VD pharmacokinetics were evaluated in RMs after a single intravenous injection at the doses of 20 (9051 and 9071) and 40 mg (9091 and 9052). Sera concentration of Q-VD was assessed by liquid chromatography-mass spectrometry (HPLC-MS/MS), sampled at different time point after injection. Half-life ($T_{1/2\beta}$) was 3.38, 3.89, 3.57 and 4.21 hrs, respectively. The AUC_{last} was 86.69, 79.42, 144.7 and 252.4 $\mu\text{g/ml}$, respectively. (B) Tissue concentration in LNs was measured after 4 hrs in the same animals. (C) Biochemical parameters including urea, ALAT, ASAT and creatinine were measured in the sera of Q-VD treated RMs at the dose of 20 and 40 mg in comparison to placebo alone (diluted DMSO). Dashed lines represent the normal values. Only ASAT levels were higher than the normal value peaking at 8 hrs but similar in treated and non-treated RMs. Only RM #9052 shows higher level of creatinine, early after injection consistent with the PK.



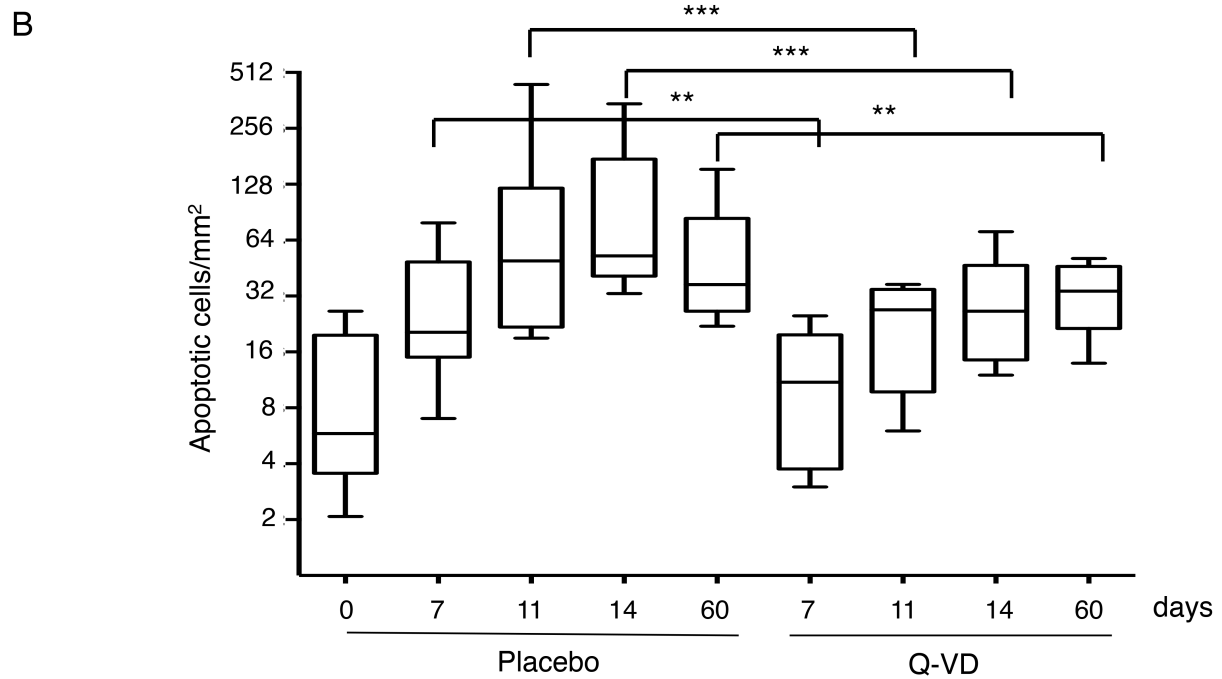
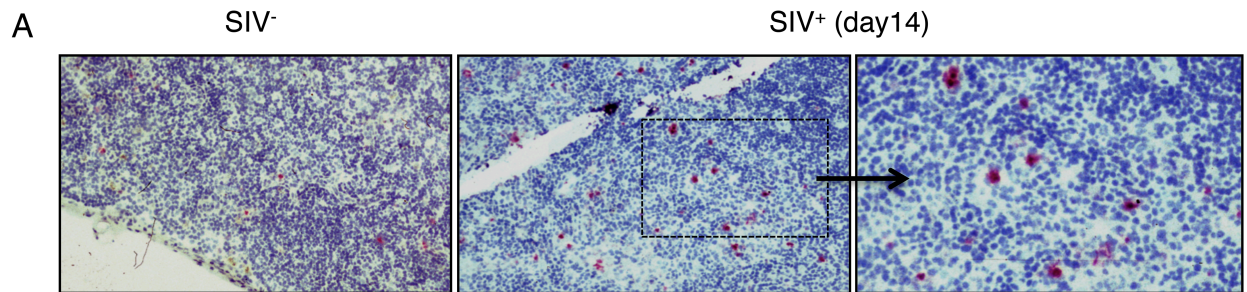
Supplemental Figure 4: Q-VD study design and samplings.



Supplemental Figure 5: Hemogram of SIV-infected RMs. Red blood and platelet counts and hemoglobin concentration was quantified in untreated (Placebo, n=11) or Q-VD treated RMs (n=6). Box indicates period of treatment. No difference is observed between untreated and treated monkeys.

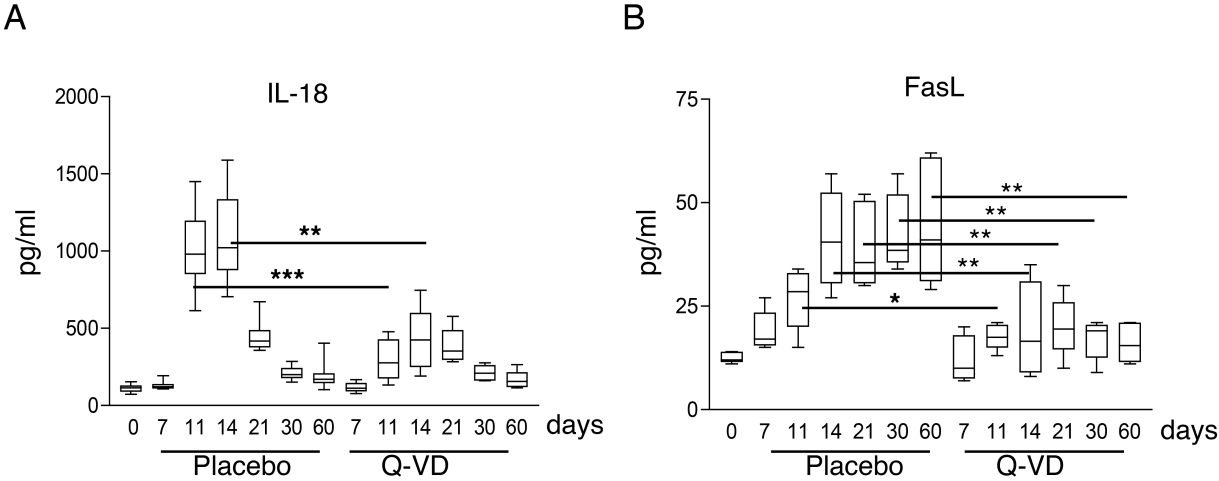


Supplemental Figure 6: Immunohistochemical analysis of apoptotic cells in LNs of SIV-infected RMs. (A) Apoptotic cells (in red) were assessed by the TUNEL method, as previously described in Monceaux et al. (2), in LNs of a healthy and an SIV-infected RM at day 14 (magnification x200). (B) Apoptotic cell numbers in untreated (placebo, n=8) and Q-VD treated SIV-infected RMs (n=6) at different time points post-infection. The error bars represent standard deviations and statistical significances were assessed using the Mann–Whitney *U*-test comparing at each time point the two groups.

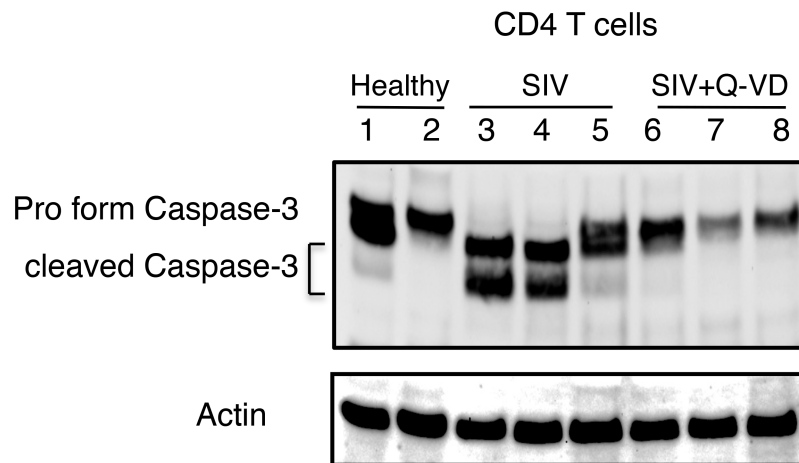


Supplemental Figure 7: Q-VD-OPH reduces *in vivo* inflammatory responses in SIV-infected RMs.

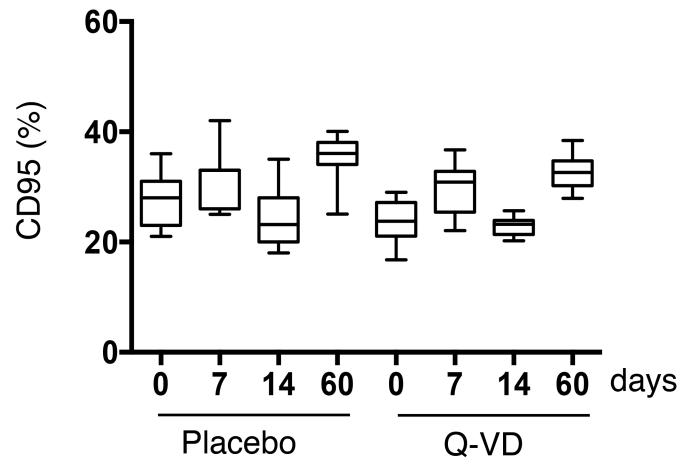
The levels of (A) IL-18 and (B) FasL were measured in the sera by ELISA at different time point post-infection. Statistical analysis was assessed using the Mann–Whitney *U*-test (0.01<***<0.05; 0.001<****<0.01; *****<0.001; ns, not significant).



Supplemental Figure 8: Cleavage of caspase-3 in purified CD4 T cells. CD4 T cells at 6 months post-infection were isolated from peripheral blood of healthy (lanes 1, 2), SIV-infected RMs (lanes 3, 4, 5) and SIV-infected RMs treated with Q-VD-OPH (lanes 6, 7, 8). Cells are lysed in Nonidet P-40 buffer (1% NP-40, 50 mM Tris-HCl (pH 7.4), 150 mM NaCl). Lysates were subjected to electrophoresis in NUPAGE 4–20% polyacrylamide gels (Invitrogene). The proteins were transferred to polyvinylidene difluoride membranes (Amersham Bioscience) and then incubated with primary antibodies. The primary antibodies used for western blotting were a rabbit polyclonal anti-caspase-3 (PharMingen, San Diego, CA), and a mouse anti-tubulin (Sigma-Aldrich). The proform and the active form of caspase-3 (32 kDa, and 20/17 kDa, respectively) are shown. Actin was used a control of loading.

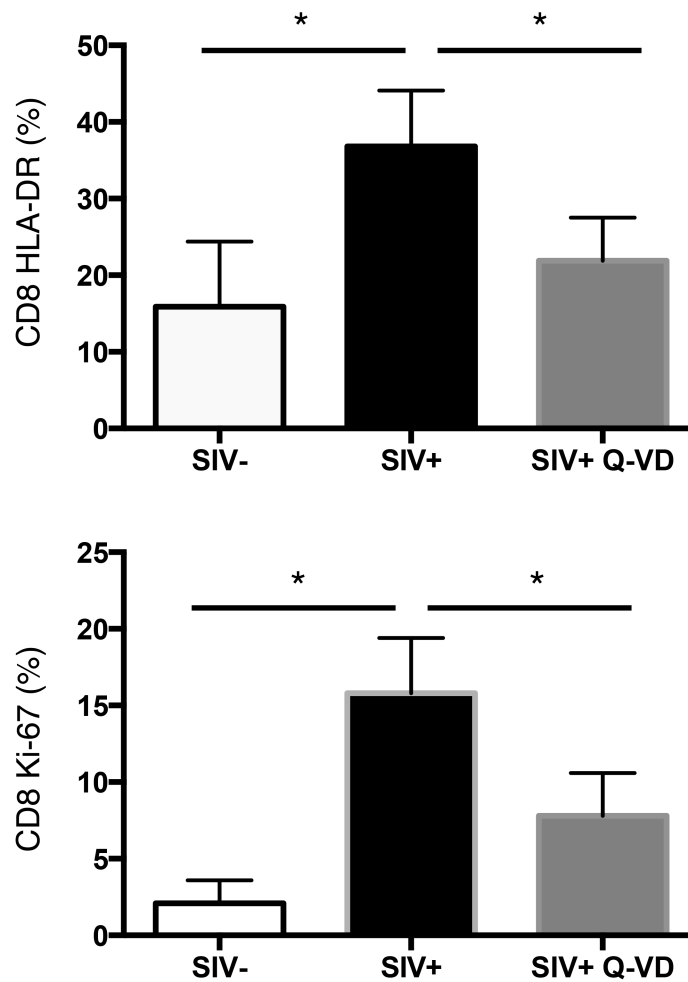


Supplemental Figure 9: CD95 expression of LN CD4 T cells. Cells isolated from LNs of untreated (placebo, n=8) and Q-VD treated SIV-infected RMs (Q-VD, n=6) at different time point post-infection were stained using CD3, CD4, CD95 mAbs and analyzed by flow cytometry as previously described (3). The percentages of CD4 T cells expressing CD95 is shown, and no statistical significance was observed.



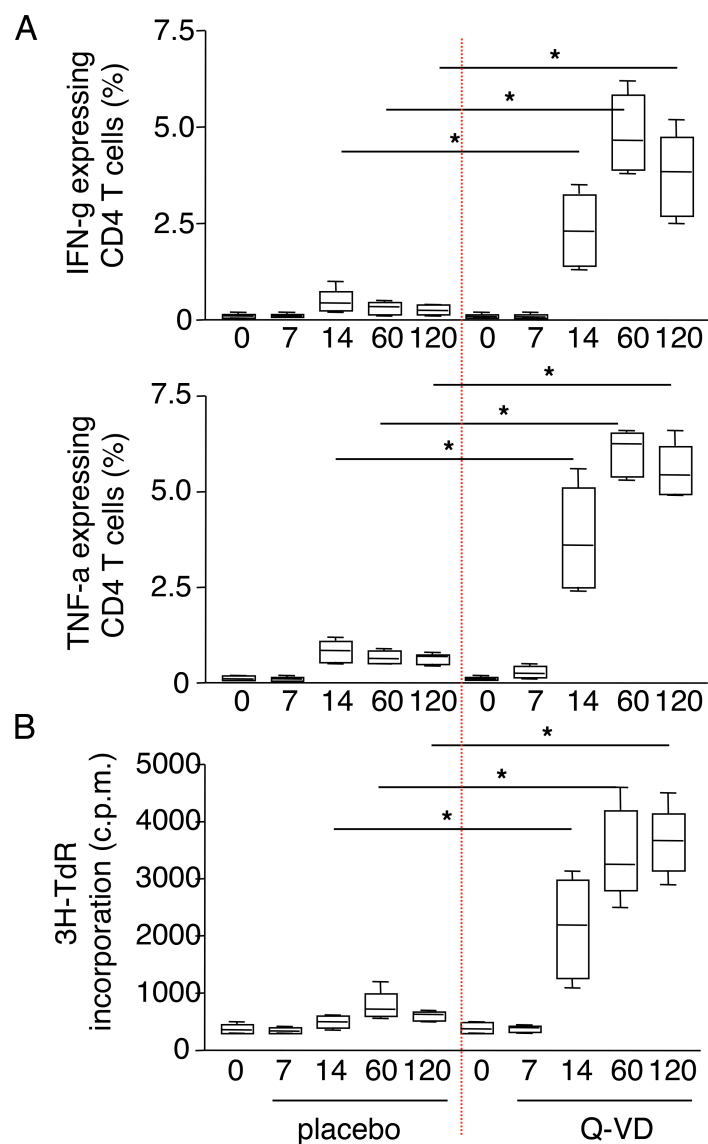
Supplemental Figure 10: Q-VD-OPH treatment reduces CD8 T cell activation in SIV-infected RMs.

The percentages of CD8⁺ T cells expressing (Top) HLA-DR, and (bottom) Ki67 were assessed by flow cytometry from blood of either healthy RMs (n=6), untreated SIV-infected RMs (SIV+, n=8) or Q-VD-OPH-treated (SIV+Q-VD, n=6) RMs at day 180 post infection. Statistical analysis was assessed using the Mann–Whitney *U*-test (p, *<0.05).

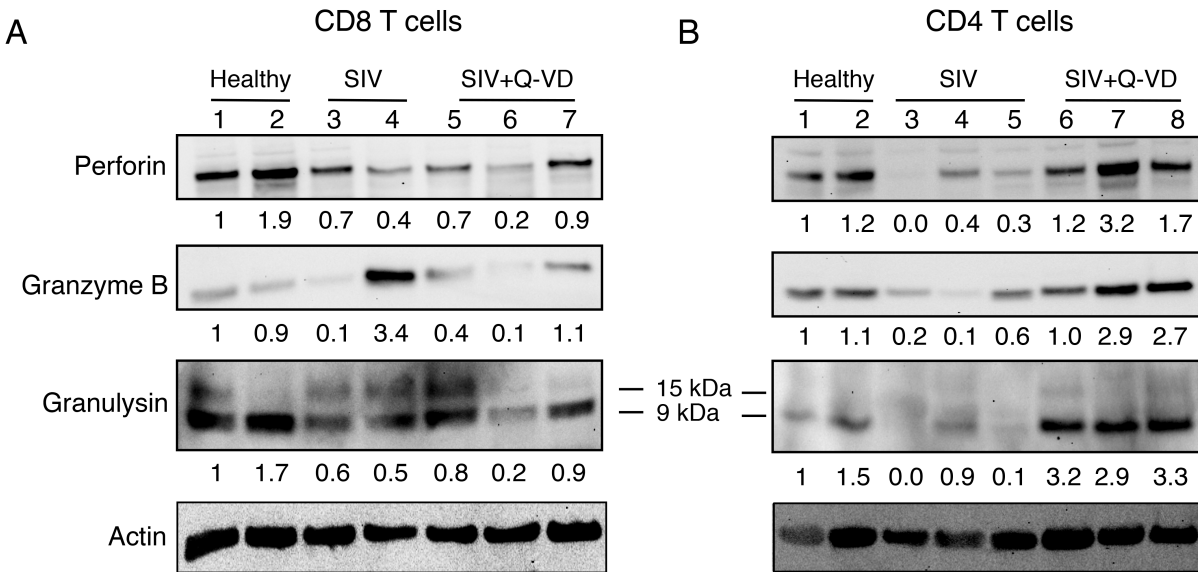


Supplemental Figure 11: Q-VD-OPH increases specific T cell responses in SIV-infected RMs.

(A) PBMC were isolated on gradient density at different time points post infection and then restimulated with HIV-2 antigens. After overnight culture, the expressions of IFN- γ and TNF- α were measured by flow cytometry after intracellular cellular staining of CD3⁺CD4⁺ T cells of either untreated (placebo, n=6) or Q-VD-OPH-treated RMs (n=6) at different time points post infection. (B) At day 6, T cell proliferation was measured by [3H]-thymidine incorporation. The ddi was added in the culture to inhibit viral replication. Background of T cell proliferation was around 500 cpm. Statistical analysis was assessed using the Mann–Whitney test and a three folds increase over the background was considered to be specific.



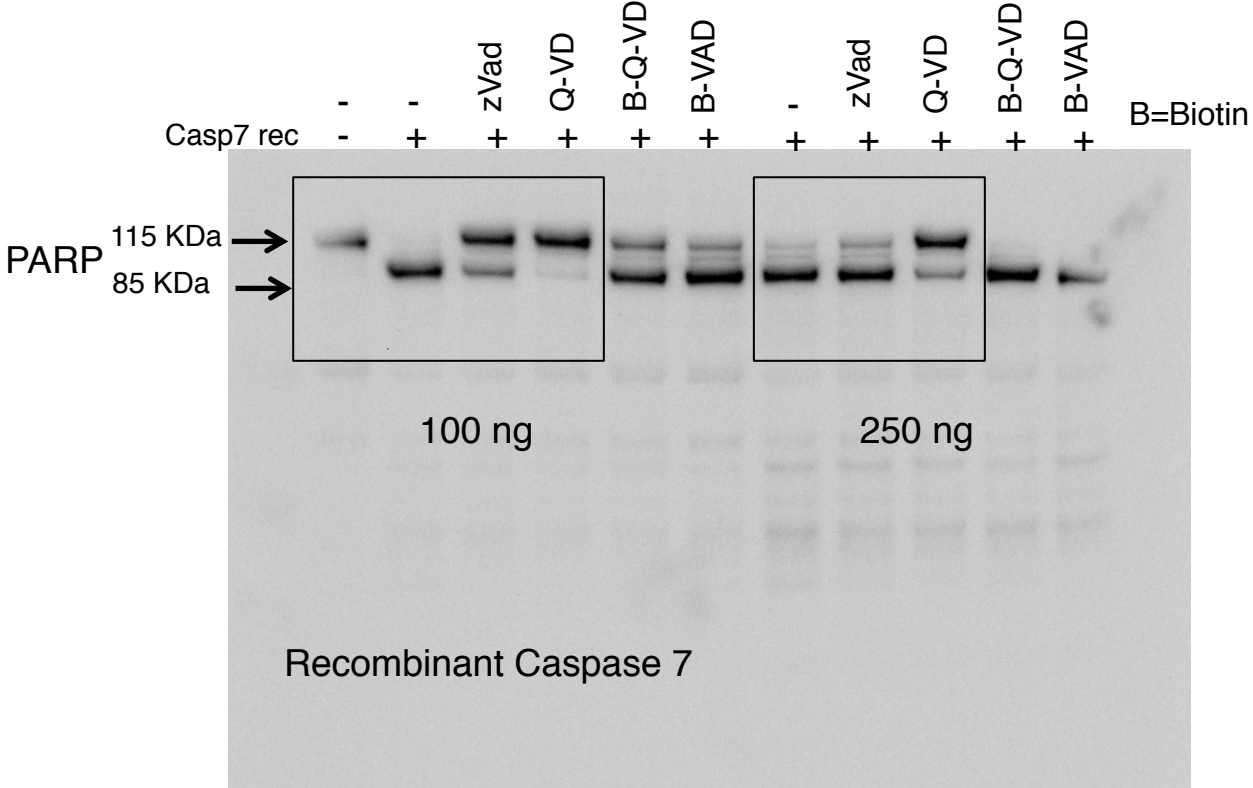
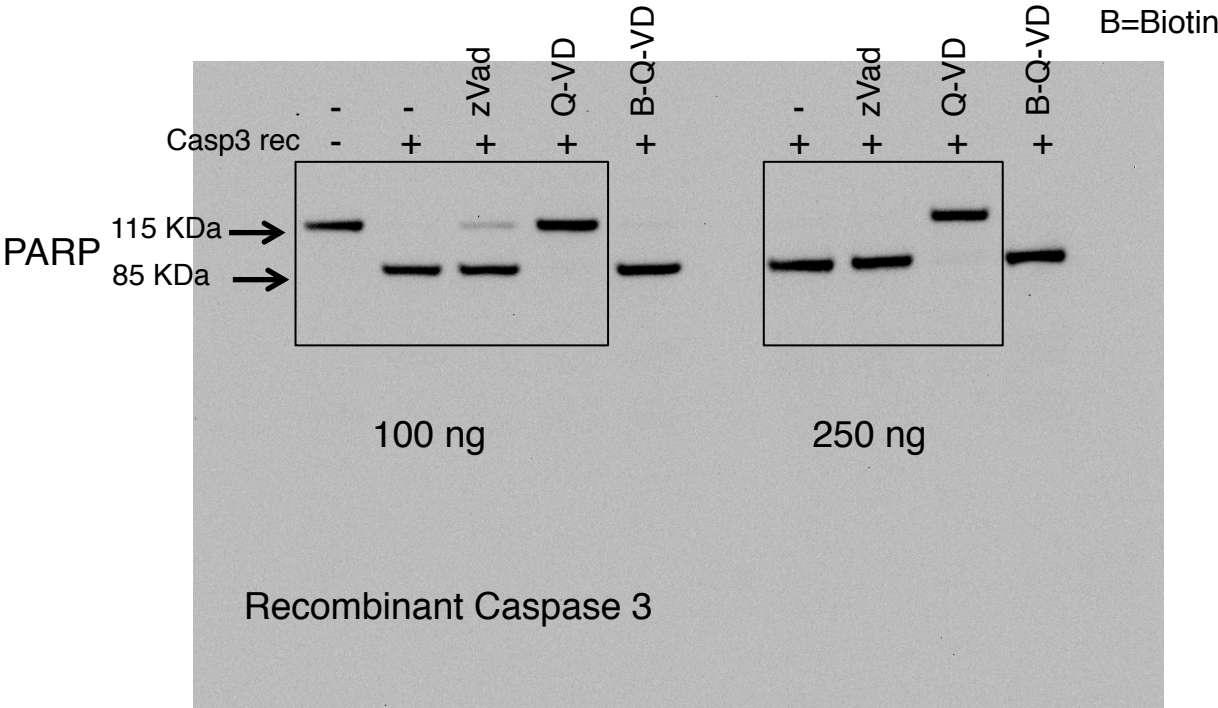
Supplemental Figure 12: Expression of cytolytic molecules in T cells of SIV-infected RMs. (A) Expression of Perforin, Granzyme B and Granulysin in purified (A) CD8 and (B) CD4 T cells isolated from peripheral blood of healthy (lanes 1, 2), SIV-infected RMs (lanes 3, 4, 5) and SIV-infected RMs treated with Q-VD-OPH (lanes 6, 7, 8). Cells were isolated at 6 months post-infection. Actin was used a control of loading. Values are compared to lane 1 after actin normalization.



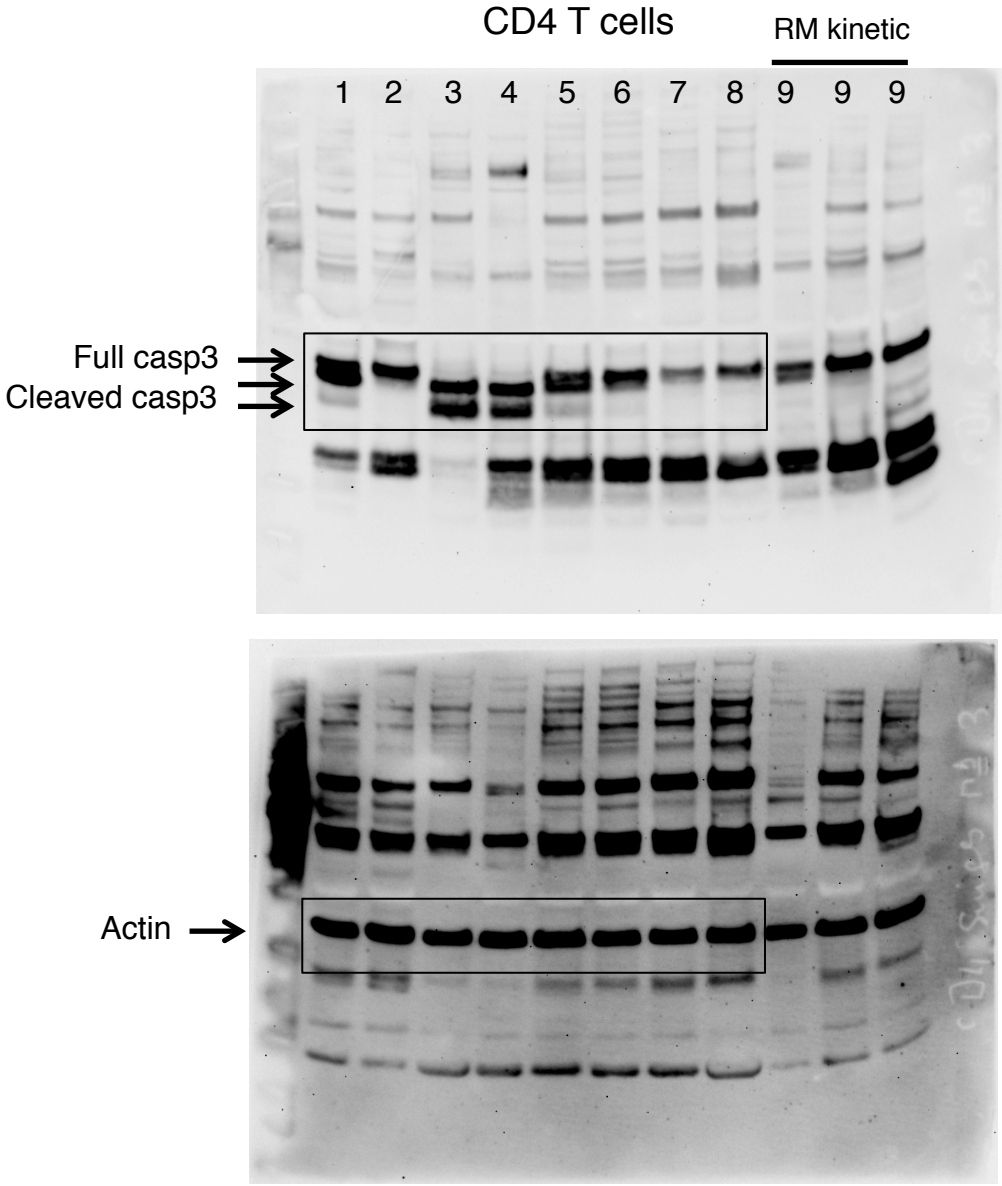
References

1. Letvin NL, Eaton KA, Aldrich WR, Sehgal PK, Blake BJ, Schlossman SF, King NW, and Hunt RD. Acquired immunodeficiency syndrome in a colony of macaque monkeys. *Proceedings of the National Academy of Sciences of the United States of America*. 1983;80(9):2718-22.
2. Monceaux V, Estaquier J, Fevrier M, Cumont MC, Riviere Y, Aubertin AM, Ameisen JC, and Hurtrel B. Extensive apoptosis in lymphoid organs during primary SIV infection predicts rapid progression towards AIDS. *Aids*. 2003;17(11):1585-96.
3. Viollet L, Monceaux V, Petit F, Ho Tsong Fang R, Cumont MC, Hurtrel B, and Estaquier J. Death of CD4+ T cells from lymph nodes during primary SIVmac251 infection predicts the rate of AIDS progression. *Journal of immunology*. 2006;177(10):6685-94.

Full unedited gel for Supplemental Figure 1

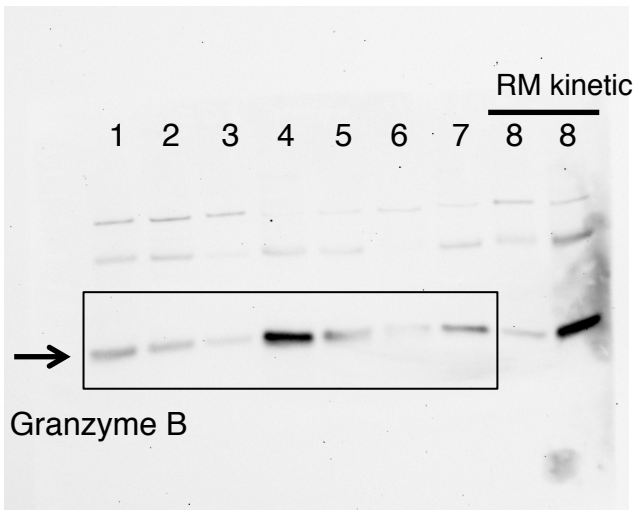


Full unedited gel for Supplemental Figure 8

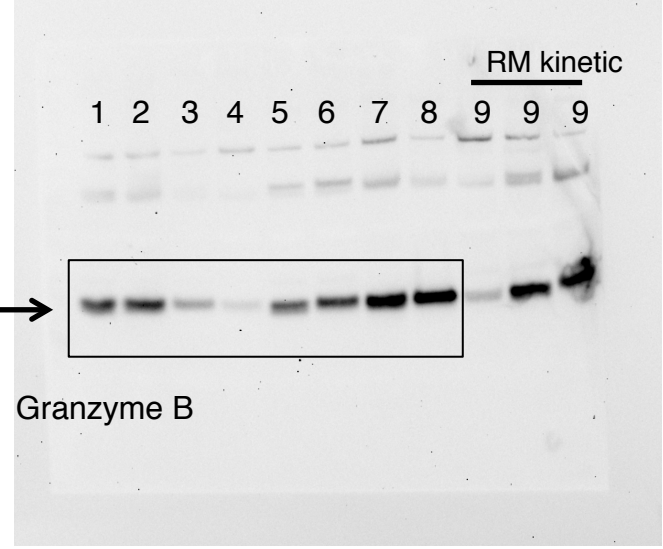


Full unedited gel for Supplemental Figure 12

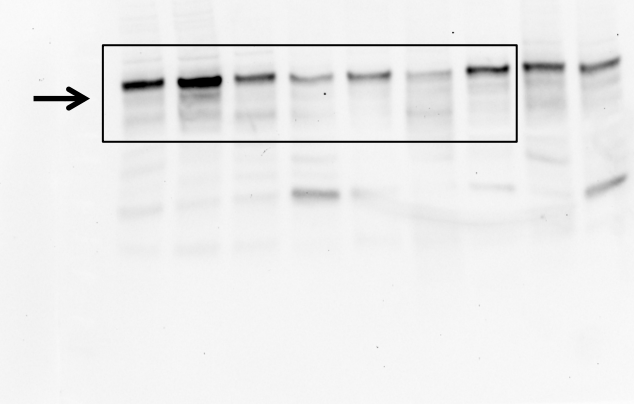
CD8 T cells



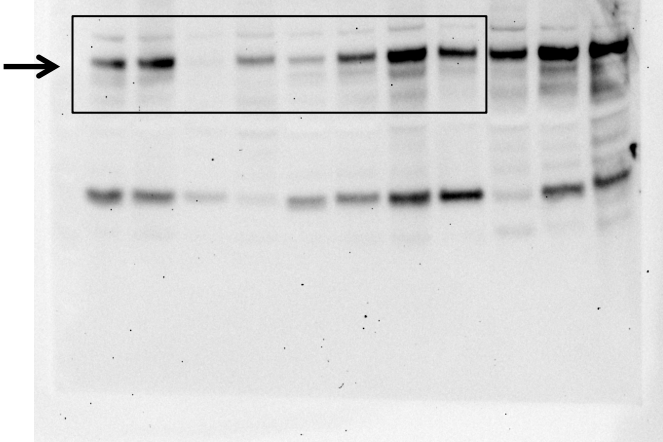
CD4 T cells



Perforin



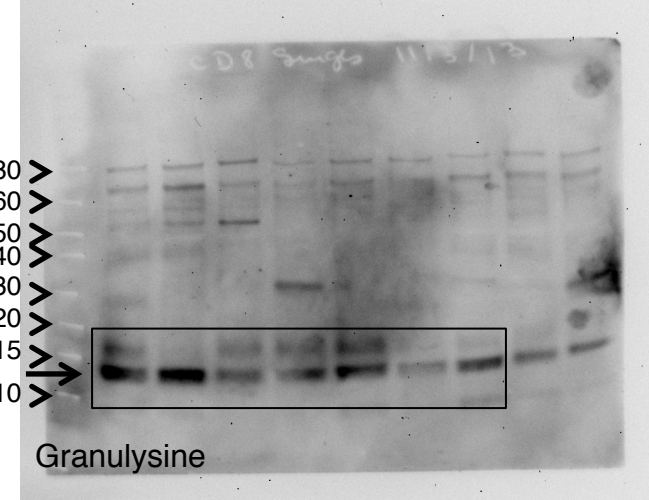
Perforin



CD8 surge 11/3/13

80
60
50
40
30
20
15
10

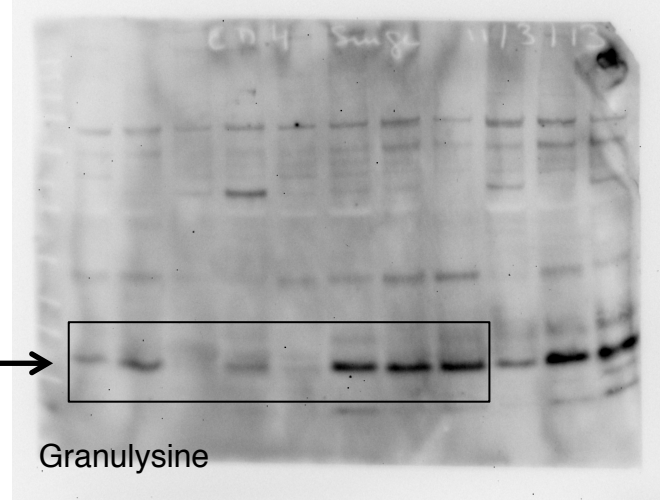
Granulysin



CD4 surge 11/3/13

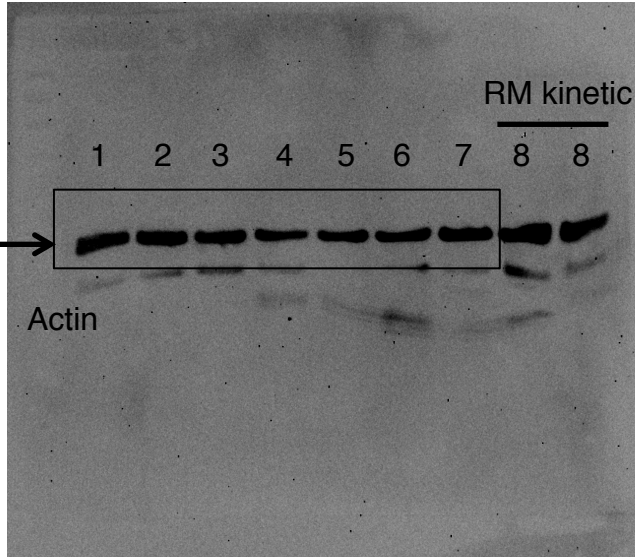
→

Granulysin



Full unedited gel for Supplemental Figure 12

CD8 T cells



CD4 T cells

